VERTICAL VARIATION IN DIFFUSION COEFFICIENT WITHIN FIXED BED RIVER SEDIMENTS

Ian Chandler[1], Jonathan Pearson[1], Ian Guymer[1] & RogerVan-Egmond[2]

[1]School of Engineering, University of Warwick, England, Coventry, CV4 7AL

[2]Unilever Safety & Environmental Assurance Centre (SEAC), England, Colworth Science Park, Sharnbrook, Bedfordshire

E-mail: I.D.Chandler@warwick.ac.uk

Abstract

This paper presents experimental results quantifying the vertical variation in diffusion coefficients with depth below the sediment-water interface for one flow and sediment combination. A modified EROSIMESS-System has been used in conjunction with fibre-optic fluorometers to determine the variation. The diffusion coefficient reduces exponentially with depth below the sediment-water interface in two repeat tests with 1.85mm diameter sediment under a bed shear velocity of 0.02m/s. There is a discrepancy between the upper most coefficients calculated from the in-bed data and those calculated from the bulk exchange measurement in the water column.

Introduction

To predict the fate of chemicals released into the aquatic environment, risk assessment models based on the impact zone concept (McAvoy, et al., 2003) are increasingly being developed (Whelan, et al., 2007). As part of these models, the movement of solute chemical pollutants from the water column across the sediment-water interface, and then into the sediment bed, or vice versa, may be required. The impact zone is a region in which a rivers' ecosystem is adversely affected by the pollutants, defined by the recovery, to pre-pollutant introduction levels, of microbial respiration and nitrification (Whelan, et al., 2007; McAvoy, et al., 2003). The river ecosystem includes the macro-invertebrate benthic community which may be strongly influenced by contaminant concentrations, both in the pore water and attached to fine sediment particles (Bottacin-Busolin, Singer, Zaramella, Battin, & Marion, 2009).

Numerous studies (Elliott & Brooks, 1997; Marion, Bellinello, Guymer, & Packman, 2002; Tonina & Buffington, 2007) have shown significant mass transfer across the sediment-water interface into the hyporheic zone. However the variation in diffusion coefficient with depth below the sediment-water interface has only been studied by Nagaoka & Ohgaki (1990) and Shimizu, Tsujimoto, & Nakagawa (1990), who both used large diameter glass spheres ($d_{50} \geq 17$mm). They show a reduction in diffusion coefficient with depth, but the studies were limited to depths up to a few particle diameters below the interface.

To quantify the variation to a greater depth below the sediment-water interface (up to 76 particle diameters) a re-designed EROSIMESS-System (shortened to erosimeter), similar to that used by Chandler, Pearson, Guymer, & Van-Egmond (2010), was employed.

Theory

The erosimeter was originally designed as an in-situ erosion-meter, developed at The Institute of Hydraulic Engineering and Water Resources Management, Aachen University of Technology in Germany (IWW, RWTH). Originally deployed to determine the critical bed shear stress of sediments deposited in small hydropower plant reservoirs, it has been used to study the stabilising effect of benthic algae on cohesive sediments (Spork, Jahnke, Prochnow, & Koengeter, 1997) and the effect sediment re-suspension has on the dissolved oxygen content of river water (Jubb, Guymer, Licht, & Prochnow, 2001). For the experiments presented in this paper the original system has been re-designed for laboratory work and details are given in the experimental setup section.

The erosimeter has been used previously to quantify the diffusion coefficient across the sediment water interface (Chandler, Pearson, Guymer, & Van-Egmond, 2010). The experimentally derived coefficients were compared to coefficients from 11 previous laboratory studies through the scaling relationship (1) proposed by (O'Connor & Harvey, 2008). The scaling relationship is based on previous laboratory studies and is reproduced in Figure 1

$$\frac{D}{D'_m} = \begin{cases} 5 \times 10^{-4} Re_* Pe_K^{6/5} & \text{for } Re_* Pe_K^{6/5} \geq 2000 \\ 0 & \text{for } Re_* Pe_K^{6/5} < 2000 \end{cases} \quad (1)$$

Where: D is the diffusion coefficient, D'_m is the molecular diffusion coefficient through the sediment pore water, Re_* is the shear Reynolds number (2) and Pe_K is the permeability Péclet number (3).

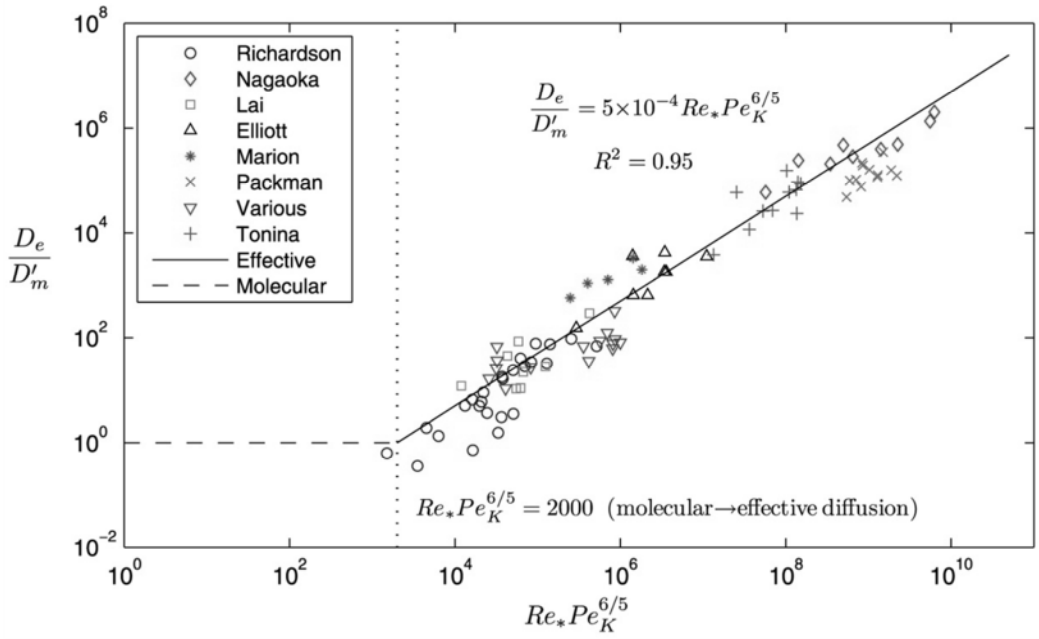

Figure 1: Effective diffusion scaling relationship plotted with experimental data used to derive the relationship (O'Connor & Harvey, 2008).

$$Re_* = u_* \frac{k_s}{\nu} \quad (2)$$

Where: u_* is the bed shear velocity, k_s is the roughness height and ν is the kinematic viscosity.

$$Pe_K = u_* \frac{\sqrt{K}}{D'_m} \quad (3)$$

Where: K is permeability.

The data used by O'Connor & Harvey (2008) resulted from several different experimental setups. All studies used re-circulating flumes, but the initial location of the solute tracer and the measurement system (either in-bed or water column) was different. This resulted in several different equations being used to analyse the data, however they all used the same general methodology. For a temporal concentration profile obtained from an instruments positioned within the water column and tracer initially located in the sediment pore water (in-bed), O'Connor & Harvey (2008) used (4) to calculate the diffusion coefficient across the sediment-water interface (D). The same approach was used by Chandler, Pearson, Guymer, & Van-Egmond (2010) and others.

$$D = \left(\frac{\sqrt{\pi}}{2C_{0,s}} \frac{\mathrm{d}M_w}{\mathrm{d}t^{1/2}} \right)^2 \quad (4)$$

Where: $C_{0,s}$ is the initial solute concentration within the sediment pore water, $\mathrm{d}M_w/\mathrm{d}t^{1/2}$ is the initial slope taken from the temporal concentration profile, where M_w is the accumulated mass of solute tracer in the water column and $t^{1/2}$ is the square root of time. O'Connor & Harvey (2008) do not specify what portion of the profile corresponds with the initial slope.

The experimental setup described below, has solute tracer initially placed in the sediment pore water, clean water in the water column above, five instruments positioned vertically in the bed and one in the water column. This results in several temporal concentration profiles at different depths below the sediment-water interface and one from the water column. Figure 2 shows the expected temporal concentration profiles, generated using a numerical one-dimensional diffusion model. The vertical diffusion coefficient varies with depth and the profiles are taken from spatial points that correspond to the instrument locations in the experimental setup. Plotting the x-axis as $t^{1/2}$ allows both the rapid exchange near the sediment-water interface (e.g. 15mm below the interface) and the slow exchange furthest away (e.g. 151mm) to be seen together.

The temporal concentration profiles from the water column in this study have been analysed using (4). However the same methodology cannot be applied to the in-bed profiles. The in-bed profiles were analysed using the methodology and equations described in Nagaoka & Ohgaki (1990). The method uses the upper profile, $f(t)$, (such as 49mm below the sediment-water interface) in a pair to predict the lower profile (C_A), that should match that measured, e.g. at 83mm below the interface (Figure 2). The diffusion coefficient (D_1) is optimised within (5) so C_A gives the best fit to the measured lower profile. This process allows the average coefficient for the region between the two profiles to be obtained.

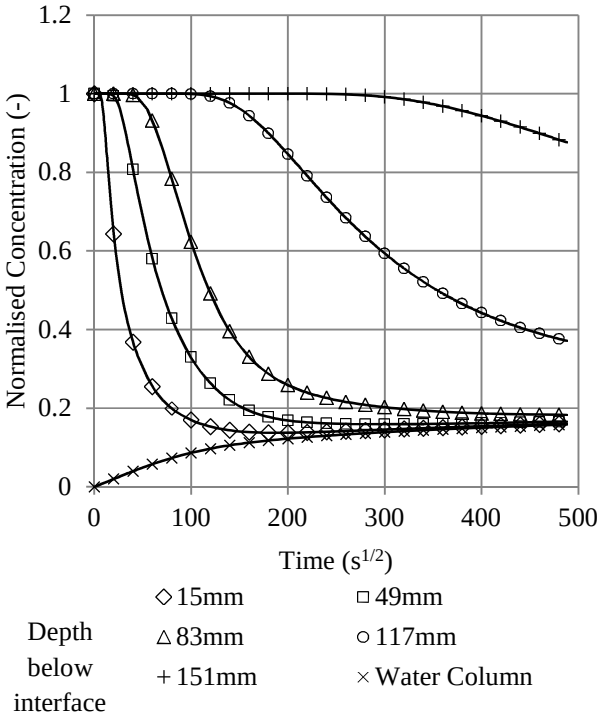

Figure 2: Expected temporal concentration profiles from the experimental setup used (generated using a 1D diffusion model)

$$C_A[f(t), D_1, D_2] = C(t, L) = \frac{L}{(a+1)\sqrt{\pi D_1}} \times \int_0^t \frac{f(t)}{(t-\tau)^{3/2}} \sum_{n=0}^{x} b^n(2n+1)\exp\left(-\frac{(2n+1)^2 L^2}{4D_1(t-\tau)}\right) \mathrm{d}\tau \quad (5)$$

Where: t is time, L is the distance between the two profiles used in the analysis, D_1 is the diffusion coefficient for the region between the two profiles, D_2 is the diffusion coefficient for the region below the lower of the profile and

$$a = \sqrt{\frac{D_2}{D_1}} \quad , \quad b = \frac{a-1}{a+1} \quad (6)$$

Equation (5) is derived from Fick's second law of diffusion, but requires the diffusion coefficient, D_2, for the region below the lower of the profile in the pair to be known. This can be obtained from analysing the profile pair below the pair currently being analysed. For example by analysing profiles from 83 and 117mm to obtain D_2 for the analysis between profiles at 49 and 83mm below the sediment-water interface. However for the lowest profile pair (e.g. 117 and 151mm) the assumption must be made that the region below the lower profile in the pair has the same coefficient as the region between the profiles. Making this assumption simplifies (5) to

$$C_B[f(t), D_1] = \frac{L}{2\sqrt{\pi D_1}} \times \int_0^t \frac{f(t)}{(t-\tau)^{3/2}} \exp\left(-\frac{L^2}{4D_1(t-\tau)}\right) \mathrm{d}\tau \quad (7)$$

where: C_B is the predicted lower profile.

The Nagaoka & Ohgaki (1990) methodology starts by analysing the lowest two profiles (e.g. 117 and 151mm), optimising D_1 in (7) so that the best fit is obtained between C_B and the measured lowest profile (151mm). The optimisation routine employed in this study uses the coefficient of determination, R_t^2, (Young, Jakeman, & McMurtrie, 1980) as the goodness of fit parameter between the measured and predicted profiles. Once the diffusion coefficient for the region between the lowest profiles has been obtained, the analysis moves to the next profile pair, second furthest from the sediment-water interface (e.g. 83 and 117mm), and uses (5) instead of (7). Again D_1 is optimised and D_2 is set using the output from the previous analysis step. This process repeats until all the profiles pairs have been analysed, finishing with the pair closest to the sediment-water interface (e.g. 15 and 49mm).

Experimental Setup

As stated in the last section the erosimeter was re-designed for these experiments. The original motor, propeller and control system were retained, but a new main section and base were designed. The primary reasons for the re-design were to improve the placement of sediment, give side access for instrumentation in the base section and incorporate an in-situ permeability test.

Figure 3 shows the re-designed erosimeter, with a flanged connection between the main section and base at the sediment-water interface, the fibre-optic fluorometers, Turner Designs cyclops 7 fluorometer, temperature sensor and outlet in the base for the permeability testing.

The main section is 300mm high with an internal diameter of 96.2mm, with a Turner Designs cyclops 7 fluorometer and temperature sensor (on opposite sides) 60mm below the top. The base section is 200mm tall and has the same diameter as the main section. Fibre-optic fluorometers are aligned vertically 15, 49, 83, 117 and 151mm below the top of the base section, also the location of the sediment-water interface.

The motor sits on top of the main section with a 260mm shaft bringing the 20mm diameter tri-bladed propeller to 40mm above the sediment-water interface. Six baffles around the circumference, at the height of the propeller, create a uniform bed shear stress at the sediment surface (Liem, Spork, & Koengeter, 1997).

The propeller speed is calibrated to the bed shear velocity (u_*) through observing the onset of sediment motion for single size sediments. Thereby obtaining the critical bed

shear stress which is used to estimate bed shear velocity by employing the Van Rijn (1984) criteria. This procedure is the same as that used by Jubb, Guymer, Licht, & Prochnow (2001).

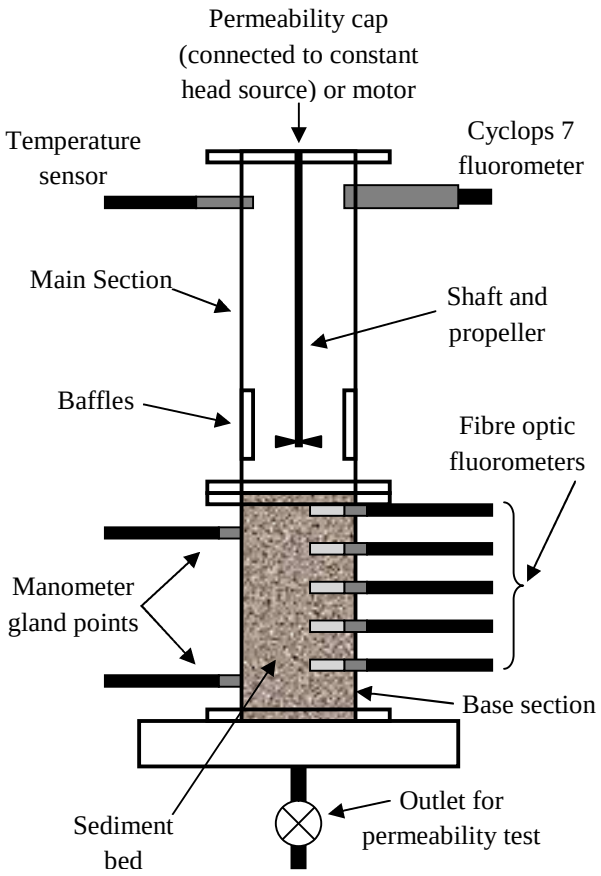

Figure 3: Schematic of erosimeter experimental setup

The base section also includes a drain so that a constant head permeability test can be conducted in-situ after solute trace experiments have been undertaken. A cap, connected to the constant head source, is placed on top of the main section, replacing the motor and housing. Manometer gland points (140mm apart) in the base are used to measure the hydraulic gradient (i) throughout the sediment bed. This gradient is used to calculate hydraulic conductivity (K_C) of the sediment using (8).

$$K_C = \left(\frac{Q}{i}\right)\left(\frac{R_t}{A_s}\right) \quad (8)$$

Where: Q is flow rate, i is hydraulic gradient (h/y), where h is the difference in manometer level and y is the distance between manometer gland points and R_t is the temperature correction factor given in British Standard 1377-5:1990.

The hydraulic conductivity is converted into a permeability (K) using (9). The equations and methodology followed are given in British Standard 1377-5:1990.

$$K = \frac{K_C \nu}{g} \quad (9)$$

Where: ν is the kinematic viscosity and g is gravity.

The fibre-optic fluorometers have a head diameter of 4mm (Figure 4) and have been developed specifically for this research. A mesh hat (30mm long by 4mm) is positioned over the end of the fibre to create a measurement volume of approximately 0.23ml. They are calibrated in-situ using a two point calibration for each test, whilst the cyclops 7 fluorometer was calibrated once before the test series.

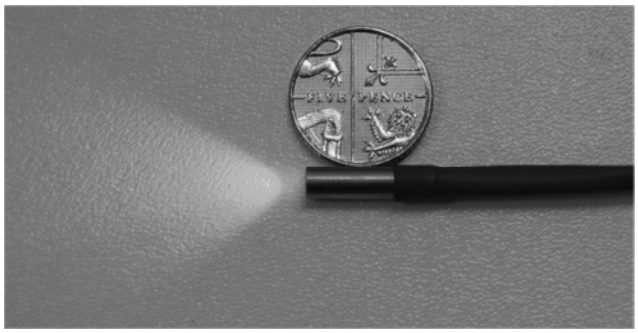

Figure 4: Photograph of fibre-optic fluorometer head and five pence piece (18mm diameter) for scale

The solute tracer used is Rhodamine WT, a fluorescent tracer developed in the 1960's specifically as a tracer (US patent 3, 367.946). In the configuration described above all the fluorometers have an accuracy of 1ppb.

The repeat tests shown in this paper were conducted on the same size sediment and under similar flow conditions. The sediment comprises glass spheres with a mean diameter (d_{50}) of 1.85mm, with 80% falling between 2.00 and 1.70mm. The porosity of the sediment was measured to be 0.39 and the permeability was found to be 2.11×10^{-9} and $2.06 \times 10^{-9}\text{m}^2$ for test 1 and 2 respectively. The bed shear velocity for both runs was 0.02m/s.

Results and Discussion

Figure 5 shows the temporal concentration profiles for all the instruments, both in-bed and water column for test 2, as well as the temperature variation throughout the test. The noise on the dye traces is most likely to be caused by temperature, as an increase in temperature will cause a decrease in fluorescence (Smart & Laidlaw, 1977). Although the temperature was recorded in the upper part of the water column during the experiments, no correction has been applied as the noise, recorded only on the lower fluorometers, did not affect the analysis. The temperature throughout the tests was 21 ± 1°C.

The increasing time it takes for mixing to start and then complete with increasing depth below the sediment-water interface is clear in Figure 5. Exchange of solute tracer from the pore water starts to occur 15mm below the sediment water interface within a minute of the test starting, whereas there is no significant mixing at 117mm until 11

hours into the test. It is also clear that equilibrium conditions have not been reached, as the trace from the instrument at 151mm below the sediment-water interface shows little change throughout the test, approximately 10% reduction. However there is enough change to allow the profile to be used in the analysis.

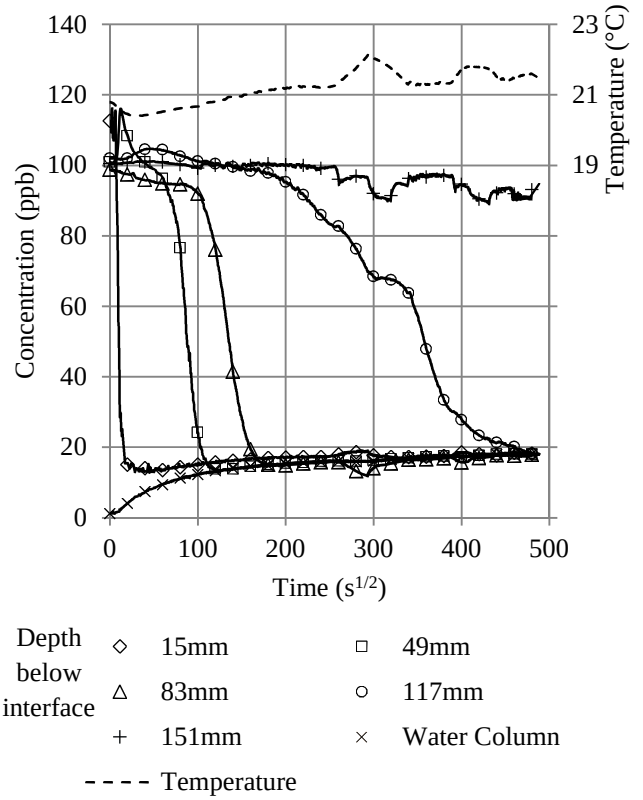

Figure 5: Concentration profiles from test 2, d_{50} of 1.85mm and u_* of 0.02m/s

The water column profiles from both tests were analysed using (4). The average diffusion coefficient for the two tests was 1.96×10^{-7}m^2/s and is approximately half the value, 3.27×10^{-7}m^2/s, predicted from the scaling relationship (1) proposed by O'Connor & Harvey (2008). The proportion of the temporal profile that should be included when calculating the initial slope used in (4) is not stated by O'Connor & Harvey (2008). A sensitivity analysis was conducted by using different percentages of the equilibrium mixing (fully mixed system) concentration as the final value included in the initial slope calculation, a range of diffusion coefficients can be calculated. This has been undertaken for test 2, and gives a range between 2.16×10^{-9}m^2/s (70%) to 4.08×10^{-7}m^2/s (2%). A comparison of the R^2 values for a linear best fit line fitted to the different portions of the data reveals that the highest R^2 value corresponds to 20% of the equilibrium concentration being used to define the initial slope. The high R^2 value indicates that a straight line best represents this portion of the data. This analysis, combined with the analysis of one-dimensional diffusion model simulations, resulted in a value of 25% of the equilibrium concentration being used to define the initial slope.

The in-bed profiles were analysed using (7) for the instrument pair 151 and 117mm below the sediment-water interface and using (5) for all the other profile pairs. Because each stage of the analysis uses two profiles, only four diffusion coefficients are obtained from the five profiles. The diffusion coefficients obtained from both tests are presented in Figure 6, along with the water column data derived coefficients.

There is close agreement between the diffusion coefficients derived from both tests at all levels within the bed, and water column. The in-bed coefficients are plotted at the midpoint between the two profiles used to obtain them. As stated previously, the analysis gives an average coefficient for the region between the two profiles. Depending on how the diffusion coefficient varies within this region, either exponentially, linearly or some other function, the average value from that variation may not occur at the midpoint. However the variation in the region between two profiles cannot be ascertained from the trace data, so the midpoint has been used.

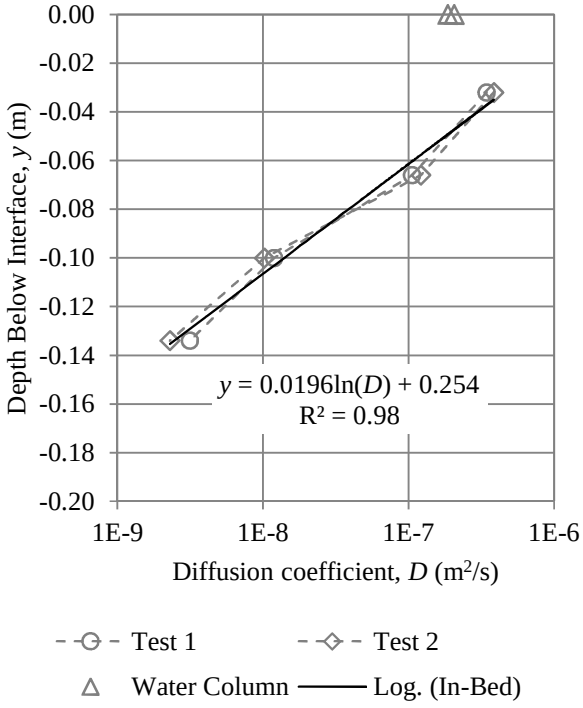

Figure 6: Variation in diffusion coefficient with depth below sediment-water interface

A best fit line has been plotted though the in-bed data in Figure 6. The line shows a logarithmic variation in depth with diffusion coefficient. This equates to an exponential change in diffusion coefficient with depth. Although this relationship is very strong and is consistent in both repeat tests, only one sediment and flow condition has been tested.

More tests with different sediment and flow characteristics are needed to determine the universal applicability of the relationship.

The average diffusion coefficient for the two tests between the profiles 15 and 49mm below the sediment-water interface is $3.64 \times 10^{-7} m^2/s$, which is very close to that predicted by the scaling relationship (1), $3.27 \times 10^{-7} m^2/s$, for the interface (O'Connor & Harvey, 2008). There is a discrepancy between the diffusion coefficient closest to the sediment-water interface derived from the in-bed data, and that derived from the water column data. The difference is $1.68 \times 10^{-7} m^2/s$, almost 50% of the in-bed value. The water column coefficient should be equal to the coefficient across the interface.

The reason for the discrepancy cannot currently be explained, but the different analysis methods applied to the in-bed data, Nagaoka & Ohgaki (1990) methodology, and the water column data, O'Connor & Harvey (2008) methodology, could account for it. The variation is within the scatter of repeat tests used by O'Connor & Harvey (2008), which span an order of magnitude, but the coefficients (Figure 6) from this study come from the same test, and the difference is repeatable. The discrepancy may primarily be from the water column data. As stated in the theory section O'Connor & Harvey (2008) do not specify what portion of the data they use to ascertain the initial slope, used in (4). This study has used 25% of the equilibrium concentration to define the last value included in the initial slope, however taking a smaller percentage does result in a higher calculated diffusion coefficient for this data set, closer to the scaling relationship predicted value.

Conclusions

There is a clear relationship shown in Figure 6 between the diffusion coefficient and depth below the sediment-water interface and good repeatability between the two tests. There is a discrepancy between the diffusion coefficient derived from the in-bed data closest to the sediment-water interface and that derived from the water column instrument. Currently this difference is not explainable, but the different analysis methodologies used on the in-bed and water column data may have an impact, particularly the percentage of the data used to define the initial slope used in (4) for the water column data. Both agree well with the interface coefficient predicted by the scaling relationship proposed by O'Connor & Harvey (2008).

To investigate the relationship between depth and diffusion coefficient further, different sediment and flow conditions need to be examined. This will indicate whether the exponential reduction seen here is universal, or if the sediment and flow conditions alter the reduction in diffusion coefficient with depth below the interface.

Acknowledgements

The authors gratefully acknowledge the Engineering and Physical Sciences Research Council (CASE/CNA/07/75) and Unilever Safety & Environmental Assurance Centre for their financial support.

References

Bottacin-Busolin, A., Singer, G., Zaramella, M., Battin, T. J., & Marion, A. (2009). Effects of Streambed Morphology and Biofilm Growth on the Transient Storage of Solutes. *Environ. Sci. Technol., 43*(19), 7337-7342.

British, Standard. (1990). *BS 1377-5: Soils for civil engineering purposes: Compressibility, permeability and durability tests.* London: British Standard Institute.

Chandler, I. D., Pearson, J. M., Guymer, I., & Van-Egmond, R. (2010). Quantifying hyporheic exchange coefficients using the EROSIMESS-system. In G. C. Christodoulou, & A. I. Stamou (Ed.), *6th International Symposium on Environmental Hydraulics. 2*, pp. 765-770. CRC Press.

Elliott, A. H., & Brooks, N. H. (1997). Transfer of nonsorbing solutes to a streambed with bedforms: Laboratory experiments,. *Water Resources Research, 33*, 137-151.

Jubb, S., Guymer, I., Licht, G., & Prochnow, J. (2001). Relating oxygen demand to flow: development of an in-situ sediment oxygen demand measurement device. *Water Science and Technology, 43*, 203-210.

Liem, R., Spork, V., & Koengeter, J. (1997). Investigations on erosional processes of cohesive sediment using an in-situ measuring devive. *Internatinoal Journal of Sediment Research, 13*(3), 139-147.

Marion, A., Bellinello, M., Guymer, I., & Packman, A. I. (2002). Effect of bed form geometry on penetration of nonreactive solute into a streambed. *Water Resources Research, 38*(10), 1209.

McAvoy, D., Masscheleyn, P., C., P., Morrall, S., Casilla, A., Lim, J. & Gregorio, E. (2003). Risk assessment approach for untreated wastewater using the QUAL2E water quality model. *Chemosphere, 52*, 55-66.

Nagaoka, H., & Ohgaki, S. (1990). Mass transfer mechanism in a porous riverbed. *Water Research, 24*, 417-425.

O'Connor, B. L., & Harvey, J. W. (2008). Scaling hyporheic exchange and its influence on biogeochemical reactions in aquatic ecosystems. *Water Resources Research, 44*, 1-17.

Shimizu, Y., Tsujimoto, T., & Nakagawa, H. (1990). Experiment and macroscopic modelling of flow in highly permeable porous medium under free-surface flow. *Hydroscience and Hydraulic Engineering, 8*(1), 69-78.

Smart, P. L., & Laidlaw, I. M. (1977). An evaluation of some fluorescent dyes for water tracing. *Water Resources Research, 13*(1), 161-172.

Spork, V., Jahnke, J., Prochnow, J., & Koengeter, J. (1997). Stabilising Effect of Benthic Algae on Cohesive Sediments. *International Journal of Sediment Research, 12*(3), 399-406.

Tonina, D., & Buffington, J. M. (2007). Hyporheic exchange in gravel bed rivers with pool-riffle morphology: Laboratory experiments and three-dimensional modelling. *Water Resources Research, 43*, W01421, 1-16.

Van Rijn, L. C. (1984). Sediment transport, part III: Bed forms and alluvial roughness. *Journal Hydraulic Engineering, 110*, 1733-1754.

Whelan, M., Van-Egmond, R., Guymer, I., Lacoursiere, J., Vought, L., Finnegan, C., Fox, K., Sparham, C., O'Connor, S., Vaughan, M. & Pearson, J. (2007). The behaviour of linear alkyl benzene sulphonate under direct discharge conditions in Vientiane, Lao PDR. *Water Research, 41*, 4730-4740.

Young, P., Jakeman, A., & McMurtrie, R. (1980). An instrumental variable method for model order identification. *Automatica, 16*, 281-294.